Original Research

PHARMACY

Application of Design of Expert software for evaluating the influence of formulation variables on the encapsulation efficacy, drug content and particle size of PEO-PPO-PEO/Poly (DL-lactide-co-caprolactone) nanoparticles as carriers for SN-38

Rozafa Koliqi[1], Pranvera Breznica[2], Arlinda Daka[1], Blerina Koshi[3]

1) Department of Clinical Pharmacy and Biopharmacy, Pharmacy Division, Faculty of Medicine, University "Hasan Prishtina", Prishtina, Republic of Kosovo

2) Department of Pharmaceutical Chemistry, Pharmacy Division, Faculty of Medicine, University "Hasan Prishtina", Prishtina, Republic of Kosovo

3) Department of Pharmaceutical Technology and Drug Control, Pharmacy Division, Faculty of Medicine, University "Hasan Prishtina", Prishtina, Republic of Kosovo

Abstract

Background and aims. Hydrophobic substances are mainly encapsulated into polymer nanocarriers in order to improve their solubility, enable their administration, at the same time to empower targeted tissue or cell specific delivery of the drug using the encapsulating vehicle as targeting and controlled release platform. 7-Ethyl-10-hydroxycamptothecin (SN-38) is an active metabolite of Irinotecan, showing 100-fold to 1000-fold higher effect than Irinotecan, but its clinical use is limited because of its extreme hydrophobicity, as it is practically insoluble in most physiologically compatible and pharmaceutically acceptable solvents.

Method. In order to fully exploit the potential of the nanoprecipitation as a method for preparation of Poly(DL-lactide-co-caprolactone)- poly(ethylene oxide) - poly(propylene oxide) - poly(ethylene oxide) (P(DL)LCL/PEO-PPO-PEO) nanoparticles and evaluate the influence of the polymer P(DL)LCL, stabilizing agent PEO-PPO-PEO copolymer (Lutrol F127) and the drug concentration (SN-38) upon drug entrapment efficiency, size and drug content, a D-optimal experimental design for response surface using Design Expert Version 9.0.4.1. software investigation was created and statistically analyzed.

Results. We have observed that at higher SN-38 concentration during the preparation procedure (nanoprecipitation, solvent diffusion method), and due to its extremely low water solubility, the drug will start to precipitate as unprotected crystals at a faster pace compared to polymer aggregation, leading to extremely low encapsulation efficacy and waste of the active compound. The most desirable combination of factor settings are SN-38 = 0.5 mg, Polymer = 5 mg and F127 = 4%.

Conclusion. This investigation utilizes the design of experiment approach and extends the primary understanding of impact of formulation development of P(DL)LCL/PEO-PPO-PEO nanoparticles as carriers for SN-38.

Keywords: research design, nanocarriers, SN-38, P(DL)LCL nanoparticles, hydrophobic and hydrophilic interactions, Irinotecan

DOI: 10.15386/mpr-1831

Manuscript received: 28.07.2020
Received in revised form: 09.04.2021
Accepted: 30.07.2021

Address for correspondence:
pranvera.breznica@uni-pr.edu

Introduction

Nanoparticles (NP), thanks to their ability to overcome multiple biological barriers to provide a therapeutic level of the drug at the site of action, have shown great potential to improve existing therapies for certain diseases [1]. Today, there are a number of examples of nanosystems for targeted delivery of anticancer drugs into solid tumours that have been registered for clinical use. Among the first are DOXIL (today there are generic doxorubicin liposomal injections), DAUNOXOME [2], whose potential in the treatment of certain types of cancer has enormously increased interest in the further development of nanoparticles and opened up new fields of research and development not only for lipids vesicular systems but also stimulated the appearance of one through specialized particles with improved in vitro and in vivo behavior such as: polymer micelles, dendrimers, conjugate drug-polymer, polypeptide and polysaccharide nanoparticles, lipid hybrids and other hybrid nanoparticles, etc. The first polymeric micellar nanosystems for clinical use such as Genexol-PM [methoxy-PEG-poly (D,L-lactide) Taxol] were approved almost 20 years after the approval of the first liposomal preparations for anticancer therapy [3].

The nanoparticle formulation process often involves the use of organic solvents, high-speed homogenization, sonication, milling, emulsification, crosslinking, evaporation of organic solvents, centrifugation, filtration, and lyophilisation [4]. During early development, at the lab or small scale, it is useful to consider what approach may be useful if the product were to be scaled up. Identification of important process conditions is critical to achieve key attributes and functions. These conditions may involve the ratio of polymers, drugs, targeting moieties, the type of organic solvent, and emulsifier/stabilizer/crosslinker, the oil-to-water phase ratio, mixing, temperature, pressure, and the pH [5,6]. Properly designed preparation process is critical step to ensure that nanocarriers will behave according to the designated use. Different methods such as: emulsification/solvent evaporation, nanoprecipitation, emulsification/solvent diffusion, salting out, dialysis, polymerization, are used for the preparation of polymeric nanoparticles and incorporating medicinal substances therein [7].

An additional issue for the manufacture of nanoparticles is environmental safety. The handling of dry materials in the nanometer size scale demands special caution as airborne nanoparticles distribute as aerosols. Lung deposition of such nanoparticles can lead to pulmonary toxicities. During dosing solution preparation, aerosolization of solutions needs to be avoided to prevent unintended exposure. Some nanoparticles are capable of penetrating the skin barrier, making dermal exposure a potential risk so adequate protection of personnel is essential [8,9]. In this respect, nanoparticles that are created entirely within a liquid environment may have significantly lower environmental impact, presumably no different from standard manufacturing of liquid pharmaceutical products.

Identifying the appropriate analytical tests to fully characterize nanomedicines, whether physical, chemical or biological, may be one of the more challenging aspects of nanomedicine development both from a technical as well as regulatory perspective [10].

While the standard analytical tests such as quantification of active and inactive ingredients, impurities, etc. in pharmaceutical products still apply, various additional techniques are employed specifically for the characterization of nanoparticle physicochemical properties. These tests involve a broad range of methods, including visualization of nanoparticles by microscopy (atomic force microscopy (AFM), transmission electron microscopy (TEM), and scanning electron microscopy (SEM)); measurement of particle size and size distribution with light scattering (static and dynamic), analytical ultracentrifugation, capillary electrophoresis, and field flow fractionation; analysis of surface charge or zeta potential; and examination of surface chemistry by X-ray photoelectron spectroscopy or Fourier transform infrared spectroscopy (FTIR). The crystalline state of drugs encapsulated in the nanoparticles can be assessed by X-ray diffraction and differential scanning calorimetry (DSC) [11].

Efficient homing after systemic delivery of nanovehicles has been limited by various reasons, but one of the most important factors is a short blood circulation time of intravenously (i.v.) administered particles, due to phagocytosis which is facilitated by the adsorption of plasma proteins to NP surfaces [12,13].

Modification of the surface of NPs with a hydrophilic layer is known to reduce opsonisation and enhance blood circulation time of NP's by providing "stealth effect", i.e., making the NP invisible to immune cell recognition [14].

Over the past two decades, a number of studies has been reported to characterize the role of hydrophilic chain conformation (i.e., brush and mushroom or train conformation) and its impact on protein corona conformation [15-17].

Generally, polyethylene glycol (PEG), Poloxamer, Poloxamine has been used widely in the development of various i.v. formulations for delivery of various active pharmaceutical ingredients, including peptides, proteins, and genes. The coating effect is highly dependent on the molecular weight (i.e. hydrophilic chain length at the particle surface), as well as on the hydrophilic polymer concentration, being the two parameters influencing the chain density and conformation at the surface of the particles [18,19].

Regarding the influence of the Mw, for example for PEG, there is a general consensus that stealth properties can be achieved by coating with a high density of PEG with Mw ranging from 2K to 10K [20-24]. A study from C. Fang et al., for passive targeting of stealth PEG poly(cyanoacrylate-

co-n-hexadecyl) cyanoacrylate (PHDCA) nanoparticles, showed that PEG surface modification of nanoparticles was able to dramatically reduce protein absorption and that the amount of protein adsorbed was directly dependent on the molecular mass of the PEG [21]. 100 to 200 nm-sized pegylated poly-lactic acid (PLA) nanoparticles showed 10-40% protein absorption, and 10 kDa was found to be the most efficient size of PEG in preventing protein absorption, compared to PEG 2 kDa and PEG 5 kDa. Approximately same results have been obtain in a study of a series of nanoparticles in sizes 160 – 270 nm prepared from diblock PEG-PLA copolymer, where the PEG Mw was varied from 2000 to 20 000, and it was found that a maximal reduction in protein adsorption was found for a PEG Mw of 5000 [22-25].

Hydrophilic chain density is commonly described in terms of the conformation that surface-bound hydrophilic chains achieve, whereas there are two main conformations such as "mushroom" or "brush" [26,27]. Mushroom conformation is dictated by having low density hydrophilic chain coverage, where the chains are not fully extended away from the nanoparticle surface, resulting in a thin hydrophilic layer. In the brush conformation, the chains are extending away from the nanoparticle surface, resulting in a thick layer [28].

Most of the studies show that the amount of protein bound per particle is significantly decreased with increasing hydrophilic surface density [29-31]. However, in comparison to literature, there is a study reporting protein rejection properties at much lower surface PEG density [32]. In this study nanoparticles were incubated in cell culture medium with the MH-S cells (a murine alveolar macrophage cell line) containing proteins and measured nanoparticle association with macrophages as a function of PEG surface density and time. Both PEG mushroom and PEG brush particles in the first 24 h exhibited nearly identical macrophage association and similar long-circulation profiles. In regard of this PEG mushroom and PEG brush particles show similar behavior at early time points (0.5 to 6 h) and were associated with MP-S cells 4−14 times less than non- PEGylated particles. But the difference between behaviour of mushroom and brush PEG conformations particles has been evident during the investigation of the concentration of particles in blood administered in mice, at longer times out up to 24 hours.

Despite widely accepted knowledge that PEG is extending particle circulation in vivo, there are no general standards for the surface density needed to accomplish this goal. Also, the exact mechanisms how PEGylation affects the systemic circulation time and how it enhances bioefficacy are not clearly understood, and as a consequence sometimes PEGylation may result in unexpected outcomes. This has especially been a concern during the repeated delivery of the PEGylated formulations for long-term cancer treatment [33]. For example, the effect of prolonged circulation of an i.v. injected PEGylated liposome disappeared when the second dose was injected due to the production of anti-PEGIgM, resulting in "accelerated blood clearance (ABC)" phenomenon [34]. Literature shows that the ABC phenomenon is not a universal one, i.e., it may/ or may not be observed with all PEGylated formulations. For example Professor Kiwada and his colleagues observed the ABC phenomenon in the immunostimulatory 5-cytosine-phosphate-guanine-3 (CpG) PEGylated lipoflex NP, and demonstrated that the presences of specific CpG motifs are responsible for production of anti-PEG IgM. Based on these findings they suggest that PEGylated lipoplexes containing non-CpG pDNA may achieve efficient gene expression levels in solid tumor upon repeated injection [35].

In contrary, a study of professor Ishida and his group did not show the ABC phenomenon in the PEGylated cationic liposome formulation, and they observed that two successive injections of liposomal doxorubicine allowed enhanced accumulation and broader distribution of subsequently injected (third dose) PEGylated liposomal doxorubicine in solid tumor [36].

Beside PEG, most evaluated surface coatings are amphiphilic block copolymers (poloxamers and polaxamines) which adsorb strongly onto the surface of hydrophobic core via their hydrophobic poly(propylene oxide) (PPO) centerr block and leaves the hydrophilic poly (ethylene oxide) (PEO) side-arms free to form hydrophyllic corona, providing stability to the particle suspension by a repulsion effect through a steric mechanism of stabilization and increasing the ability of NP for mononuclear phagocyte system (MPS) escape [37-44]. While low surface density of PEO chains (surface is partially covered) leads to gaps in PEO protective layer leading to free binding of opsonins to nanoparticles - higher PEO surface chain density results in the coverage of entire surface of nanoparticles, decreased mobility of the PEO chains and thus increased steric hindrance properties of the PEO layer. Actually, for the optimal surface coverage PEO protective layer chains should be in a slightly constricted configuration and at high enough density to ensure that no gaps or spaces on the particle surface are left uncovered. Further, literature data show that the strength of polymer adsorption and the resultant polymer conformation depend on the proportion and the size of both the PPO and PEO segments, as well as on forces that include the initial nanoparticle surface charge, hydrogen bonding between the polyoxyethylene ether groups and the constituent groups on the particle surface, hydrophobic forces among the polymer chains and polymer–solvent interactions [38]. Also, Li et al. pointed that, for a given triblock polymer (Poloxamer and Poloxamines) particle size showed significant influence upon surface density and hydrophylic layer thicknesses. Smaller particles were observed to adsorb fewer molecules per unit area compared to larger particles [45]. Additionally, for a particle of a given size, it is the size of the hydrophobic

center block (PPO) of the surfactant, rather than the size of its flanking tails that determines the surface density. Further, it has been demonstrated that when these prototype nanovehicles (Poloxamers and Poloxamine) were administered IV into mice, rats and rabbits, the systemic circulation have increased from 2 to 12 hours (depending on the particle size, surface hydrophobicity, copolymer type). There are many other examples that shows same result, such as a biodistribution study of polystyrene nanoparticles (Moghimi with colleagues) that shows the significant impact of Poloxamine 908 in increasing the circulation time of NP, compare with uncoated one. Same result has shown carbon nanotube (CNT) and silicon dioxide (SiO2) nanoparticles coated with Pluronics F127 [46].

Although there is significant improvement in managing in vivo particle behavior by hydrophilic coating, still remains the lack of general standards in term of what surface density and conformation is needed to extend particle circulation in vivo, and this comes due to a deficiency of methods for efficient hydrophilic corona evaluation.

Also, while the formation of the protein corona in real biological conditions is a process that cannot be controlled and completely prevent by hydrophilic corona formation, it is of utmost importance to evaluate the influence of the qualitative and quantitative composition of the proteins on NP in vivo behavior, in order to build a rational approach in the formulation of so called "stealth nanoparticles" that would provide long circulation, efficient homing, minor side effects and targeted release of active substances.

Taking into account the above, and in order to contribute to solving the problems of drug hydrophobicity, in this investigation will be designed P(DL)LCL/PEO-PPO-PEO polymer system whereas anticancer agent 7-Ethyl-10-Hydroxycamptothecin (SN-38) was incorporated, and all significant variables (polymer, SN-38 and stabilizing agent concentration) will be statistically analyzed and optimized as well. Therefore D-optimal design investigation was created to fully evaluate the factors influencing the particle size (PS), efficacy of encapsulation (EE) and drug content (DC), as well as to define the design space towards higher drug loading, efficacy of encapsulation and appropriate particle size. Analyses were performed in Design-Expert 9.0.4.1, produced by Stat-Ease, Inc.

Methods

Poly(DL-lactide-co-caprolactone)copolymer (LA:CL 10:90, Mw 77799 Da) was purchased from Akina, Inc. USA. 7-Ethyl-10-hydroxycamptothecin was obtained from Xi'AnGuanyu Bio-tech Co., China. Poly(ethylene oxide) - poly(propylene oxide) - poly(ethylene oxide) copolymer (Lutrol F127) was kindly donated by BASF, Germany. All other materials were used as received.

The P(DL)LCL nanoparticles were prepared using the nanoprecipitation method. Polymer and SN-38 were dissolved in 5ml tetrahydrofuran (THF). The organic solution was then added drop wise into the 50 ml aqueous phase containing the hydrophilic surfactant Lutrol F127 under continuous stirring at a speed of 6500 rpm / min using magnetic stirrer. THF was removed from nanodispersion overnight under continues stirring and afterwards the nanodispersion was filtered through 0.45µm regenerated cellulose membrane filters (MiniSart RC 15, Sartorius, Germany) and concentrated to volume of 2mL using ultrafiltration tubes with a pore size of 1000KDa (Vivaspin 20 1000KDa, Sartorius, Germany) in a centrifuge at 3500rpm and 4°C (Centurion Scientific, UK).

Hydrodynamic diameter (Rh) of the nanoparticles was determined by dynamic light scattering at an angle of 173° using Zetasizer Nano ZS (Malvern Instruments, UK). Drug content and efficacy of encapsulation were calculated using the following equations:

$$DC = \frac{\text{Amount of active substance in NP}}{\text{Total amount of polymer}}\ x\ 100$$

$$EE = \frac{\text{Amount of active substance in NP}}{\text{Total amount of active substance}} \text{x } 100 \quad [47].$$

D-optimal response surface design was used to evaluate the influence of formulation variables (polymer, drug and stabilizing agent concentration), their second order and quadratic interactions upon particle size, efficacy of encapsulation and drug content. To optimize the formulation variables (polymer, SN-38 and F-127) with respect to optimal P(DL)LCL/PEO-PPO-PEO nanoformulation (high drug content, high efficacy encapsulation and smaller particle size), design of experiments (DOE) and data analysis was carried out with the help of statistical software Design-Expert (Version 9.0.4.1). Summary of factors are presented in table I. D-optimal design matrix with all values and obtained results is presented in table II.

Prior to analyzing the dataset, the evaluation tool was used to confirm that all required model terms (main effects A, B and C, two-factor interactions (2FI) AB, AC and BC and three-factor interaction ABC) could all be estimated. A three level factorial design was used to achieve all possible combinations of input variable that are able to optimize the response within the region of 3-D space. The R-Squared value for each response was used to indicate the proportion of variance in the response that has been explained by the model (0-1 scale). A value close to 1 suggests that the model has captured most of the variability observed in the experimental results.

Table I. Summary of factors.

Design Summary										
Factor	Name	Units	Type	Subtype	Minimum	Maximum	Coded	Values	Mean	Std. Dev
A	SN-38	mg	Numeric	Continuous	0.5	1.5	-1.000=0.5	1.000=1.5	1.01471	0.390018
B	Polymer	mg	Numeric	Continuous	5	10	-1.000=5	1.000=10	7.27941	1.83474
C	F127	%	Numeric	Continuous	1	4	-1.000=1	1.000=4	2.41176	1.12132

Table II. D-optimal design matrix with all values and obtained results.

Study	Run	Factor 1 A: SN-38 mg	Factor 2 B: Polymer mg	Factor 3 C: F127 %	Response 1 EE %	Response 2 DC %	Response 3 PS nm
3	1	0.5	10	1	10.64	0.532	188
4	2	1.5	10	1	3.04	0.456	195
7	3	1	7.5	1.75	21.2	2.83	159
12	4	1	7.5	3.25	33.9	4.52	160
2	5	1.5	5	1	2.42	0.726	189
6	6	0.75	7.5	1.75	16.93	1.7	190
5	7	1	6.25	1.75	12.34	1.97	181
9	8	1	6.25	2.5	17.52	2.8	187
8	9	0.75	6.25	2.5	56.76	6.76	136
14	10	1.5	5	4	4.283	1.28	204
13	11	0.5	5	4	82.52	8.252	143
16	12	1.5	10	4	92.06	13.8	293
1	13	0.5	5	1	14.33	1.433	177
11	14	1.25	7.5	2.5	12.67	2.112	209
10	15	1	7.5	2.5	15.35	2.05	170
15	16	0.5	10	4	74.43	3.7	154
17	17	1.5	7.5	2.5	19.1	3.82	187

The Adjusted R-Square value adjusts the R-Squared value by considering the number of terms in the model (too many model terms can lead to extremely precise predictions for the current dataset, but a less useful predictive model). The Adjusted R-Squared value will always be less than the R-Squared value, and if the difference is greater than 0.2 then this is generally considered to indicate that too many model terms have been fitted. The Predicted R-Squared value provides a "cross-validated" measure of how predictive the model was. Each observation is iteratively excluded from the dataset, the model is re-fitted and the excluded point was predicted. A large difference between Predicted R-Squared and the other R-Squared metrics has indicated a problem with the responses (as explained later, the responses DC and EE were better fitted after applying a square root transformation). The Residuals vs Predicted chart has been used to identify any potential outliers, which will fall outside the red warning limits. The Box-Cox Plot obtained from the establish model has been used to objectively identify the influence of formulation variables among responses such drug content, efficacy of encapsulation and particles size.

Results

The analysis of variance (ANOVA) indicated the main variables influencing the responses such us: drug content, the efficacy of encapsulation and the particle size. Also, ANOVA pointed that drug*polymer concentration, drug*stabilizing agent concentration, polymer*stabilizing agent concentration interactions, as well as drug concentration*drug concentration quadratic interaction, influenced these responses (Table III).

Efficacy of encapsulation (EE) with square root transformation

Prior to analysis, the square root of all response values was calculated (as per recommendation on Box-Cox plot) and the model was fitted to these transformed values. All model graphs are presented on the back-transformed scale.

ANOVA (Table III) confirms that, as with the non-transformed data, all main effects have an effect on EE. The transformation has resulted in all main effects being statistically significant at the 5mg level of polymer P(DL) LCL. The 2FIs AB and BC were statistically significant, suggesting that the effect of SN-38 depends on the setting of polymer P(DL)LCL and vice versa. Similarly, polymer P(DL)LCL and F127 have a dependent relationship. There appears to be no statistical evidence that SN-38 and F127 interact with one another.

Table III. Analysis of variance and descriptive statistics for response EE, DC and PS.

Source	Sum of Squares			df			Mean Square			F value			p-value Prob>F		
	EE	DC	PS	EE	DC	PS	EE	DC	PS	EE	DC	PS	EE	DC	PS
Model	92.94	9.19	15482	7	7	7	13.28	1.31	2211.78	16.31	11.68	5	0.0002	0.0007	0.0145
A-SN-38	16.32	0.04	6620.62	1	1	1	16.32	0.04	6620.62	20.04	0.35	14.98	0.0015	0.5662	0.0038
B-Polymer	4.92	0.051	2065.73	1	1	1	4.92	0.051	2065.73	6.04	0.45	4.67	0.0363	0.5185	0.0589
C-F127	48.78	5.14	156.47	1	1	1	48.78	5.14	156.47	59.93	45.68	0.35	<0.0001	<0.0001	0.5665
AB	10.62	2.03	543.62	1	1	1	10.62	2.03	543.62	13.05	18.01	1.23	0.0056	0.0022	0.2961
AC	0.71	0.023	4301.98	1	1	1	0.71	0.023	4301.98	0.87	0.2	9.73	0.3754	0.6629	0.0123
BC	6.82	0.66	889.98	1	1	1	6.82	0.66	889.98	8.38	5.84	2.01	0.0177	0.0388	0.1896
ABC	6.61	1.31	861.13	1	1	1	6.61	1.31	861.13	8.12	11.68	1.95	0.0191	0.0077	0.1962
Residual	7.33	1.01	3977.42	9	9	9	0.81	0.11	441.94						
Cor-Total	100.27	10.21	19459.9	16	16	16									
R-Squared	0.9269	0.9008	0.7956												
Adj R-Squared	0.8701	0.8237	0.6366												
Pred R-Square	0.8045	0.3021	-3.1219												

The three-factor interaction ABC is statistically significant. This indicates the 2FI AB depends on the setting of factor C, and/or that AC depends on B, and/or that BC depends on A.

The most statistically important effects on EE has been identified by looking for those with the smallest p-values (indicating greatest statistical significance): main effects F127 and SN-38, plus 2FI AB. The F-value for F127 was approximately 3 times greater than the next-largest effect (F=59.93), and approximately 60 times larger than the estimate of background noise.

The Adjusted R-Squared value is less than the R-Squared value, and in this case, the difference of ≈0.05 gives no cause for concern. After applying the Square Root transformation to this response, the Predicted R-Squared value is now in close agreement to the other R-Squared values, indicating a much more predictive model.

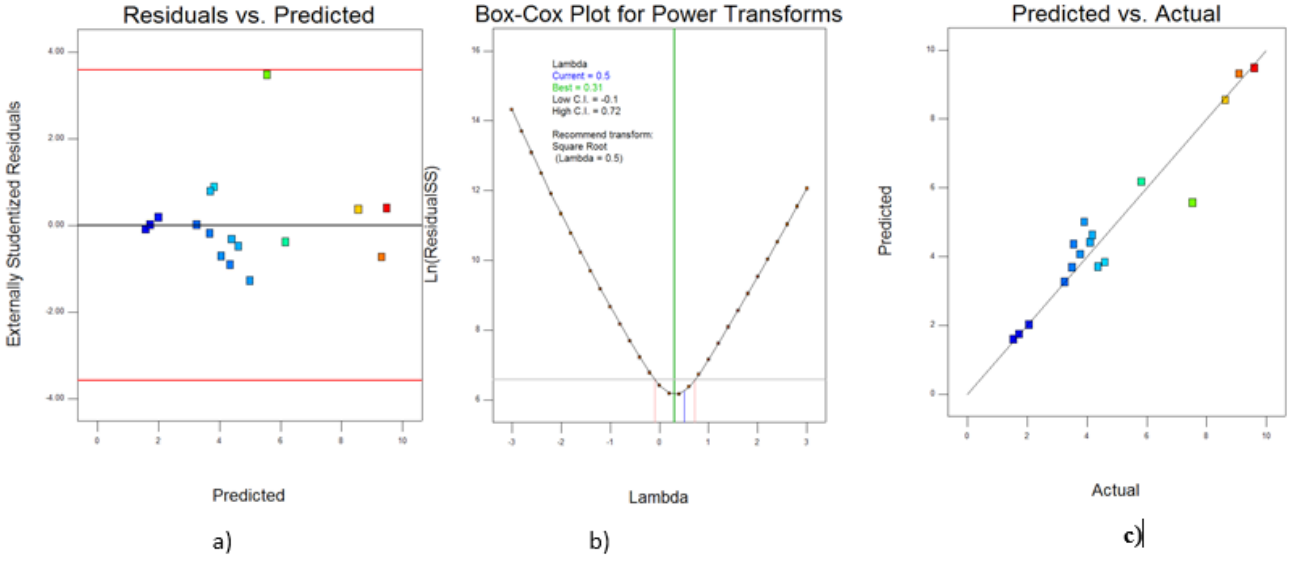

Figure 1. Response with square root transformation for efficacy of encapsulation a) Residuals vs Predicted chart, b) Box-Cox plot, c) Predicted vs Actual chart.

The Residuals vs Predicted chart for response EE, shows that there was one potential outlier in this case, run 9 (standard order 8). This particular run has not been well predicted by the model. For response EE, the Box Cox plot has confirmed that the currently applied square root transformation provides the best model fit. This plot provides a visual indication of how well the fitted model is able to predict the observed experimental results (a perfect model would result in all points appearing on the line). In this case the model appears to give reasonably good predictions, with the possible exception of run 9 (colored green). The graph shows that the actual value was 7.5, whereas the model predicted an expected value of 5.5, as presented at figure 1.

When F127=1% (low setting), the contour plot reveals little. All EE values are less than ≈15%. Increasing F127 to 2% shows an increase in EE. At this setting, the highest results are at SN-38=0.5 mg and polymer P(DL) LCL=5mg. Predicted EE is approximately 30%.When F127=3%, the EE response increases further. The optimal setting here is at SN-38=0.5 mg and polymer=5 mg. Predicted EE is just over 50%. The optimal values for EE appear to be at F127=4%, SN-38=1.5 mg and polymer P(DL)LCL =10 mg (all values at highest settings): predicted EE is approximately 90%. Alternatively, predicted EE of just over 85% can be achieved with F127=4%, SN-38=0.5 mg and Polymer P(DL)LCL =5 mg. All these are presented in figures 2 and 3.

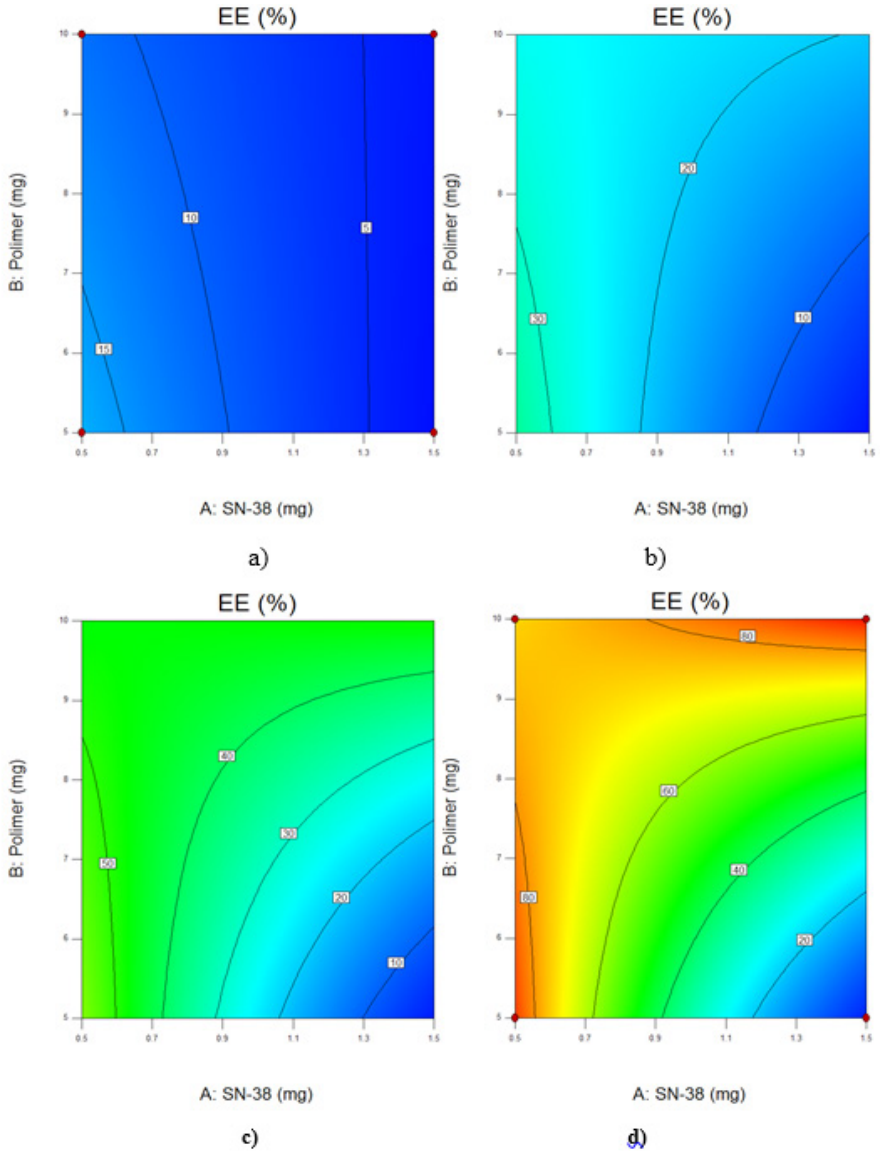

Figure 2. Response Contour Plot for efficacy of encapsulation with square root transformation at different concentration levels of Lutrol F127: a) 1%, b) 2%, c) 3%, d) 4%.

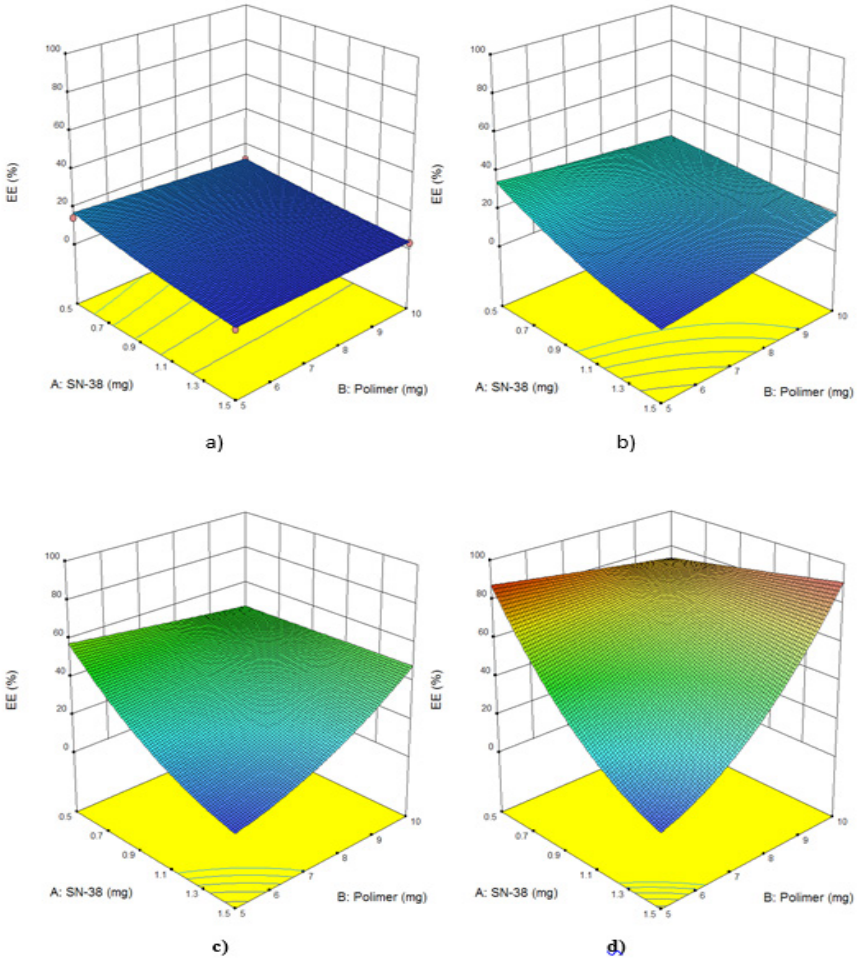

Figure 3. Response 3D Surface Plot for efficacy of encapsulation with square root transformation at different concentration levels of Lutrol F127: a) 1%, b) 2.%, c) 3%, d) 4%.

Drug content (DC) with square root transformation

Prior to analysis, the square root of all response values is calculated (as per recommendation on Box-Cox plot) and the model is fitted to these transformed values. All model graphs are presented on the back-transformed scale. ANOVA (Table III) shows that, of the main effects, only F127 has a statistically significant effect on DC.

Two-factor interactions AB and BC are statistically significant. There appears to be no statistical evidence that SN-38 and F127 interact with one another.

The three-factor interaction ABC is statistically significant. This indicates the 2FI AB depends on the setting of factor C, and/or that AC depends on B, and/or that BC depends on A.

The most statistically important effects on DC has been identified by looking for those with the smallest p-values: main effect F127 and 2FI AB.

Looking at the F-Values (a.k.a Signal / Noise ratio) shows that the effect of F127 is over 2 times greater than the next-largest effect (F=45.68), and that it is almost 50 times greater than the estimated background noise.

The Adjusted R-Squared value is less than the R-Squared value, and in this case, the difference of <0.1 gives no cause for concern.

A large difference between Predicted R-Squared and the_other R-Squared metrics indicate a problem with this response (as explained later, this is likely to be heavily influenced by outlying values).

The Residuals vs Predicted chart for response DC shows that there appears to be one potential outlier, run 9. For response DC, the Box-Cox Plot has confirmed that the currently applied Square Root transformation provides the best model fit. This plot provides a visual indication of how well the fitted model is able to predict the observed experimental results (a perfect model would result in all points appearing on the line). In this case the model appears to give reasonably good predictions, with the possible exception of run 9 (colored green), as presented in figure 4.

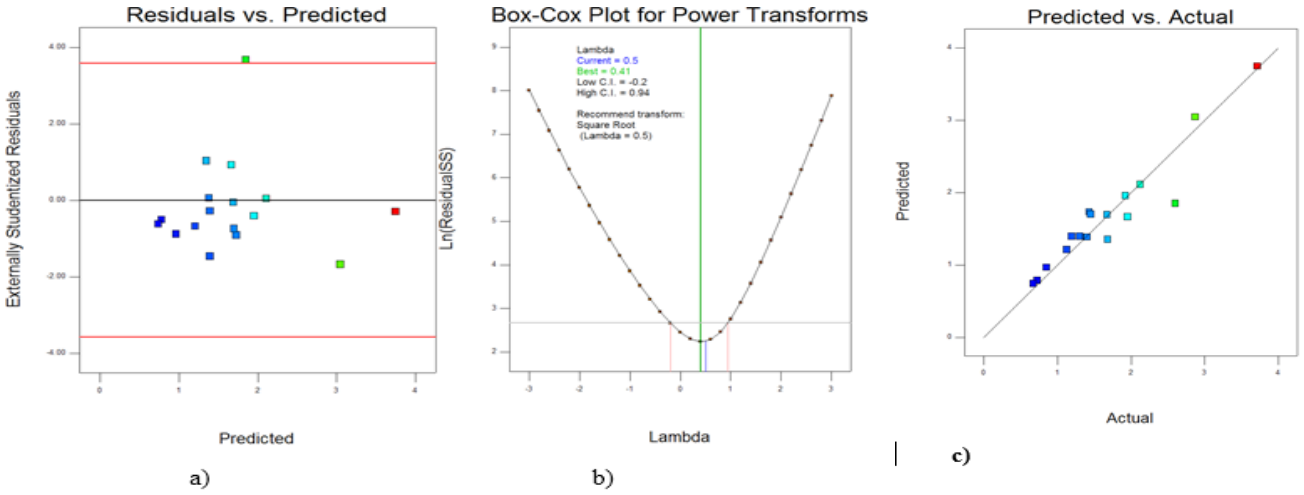

Figure 4. Response with square root transformation for drug content a) Residuals vs Predicted chart, b) Box-Cox plot, c) Predicted vs Actual chart.

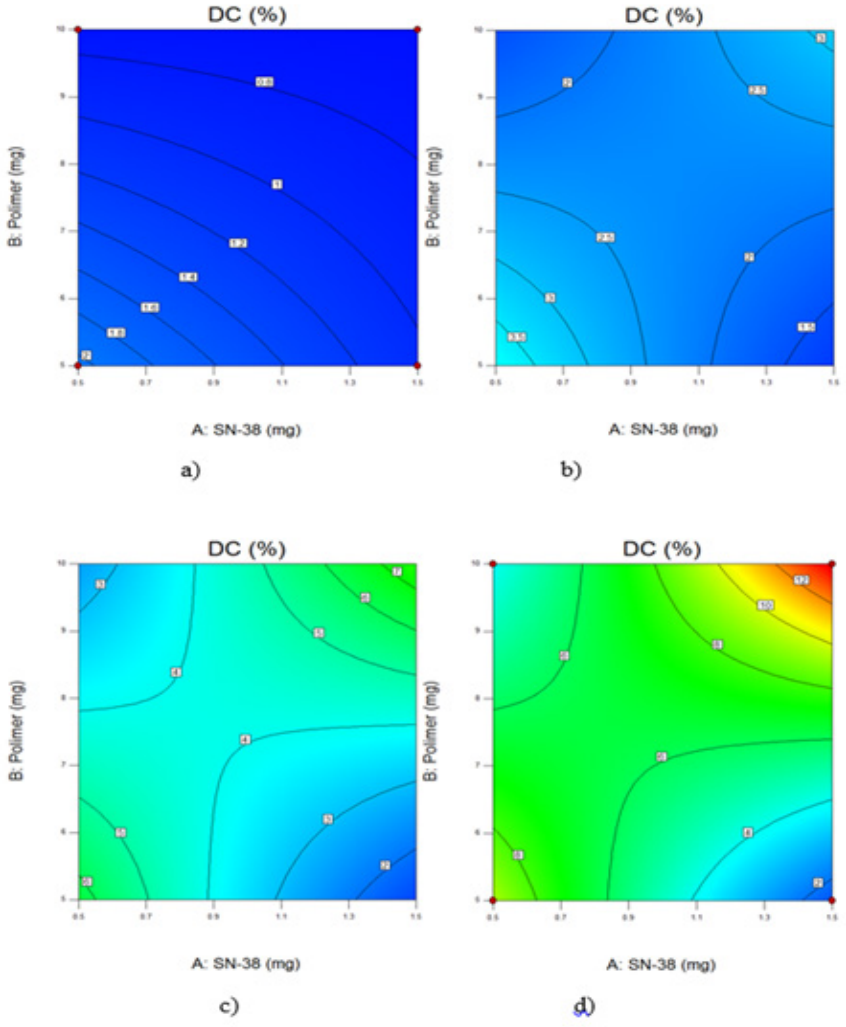

Figure 5. Response Contour Plot for drug content with square root transformation at different concentration levels of Lutrol F127: a) 1%, b) 2.%, c) 3%, d) 4%.

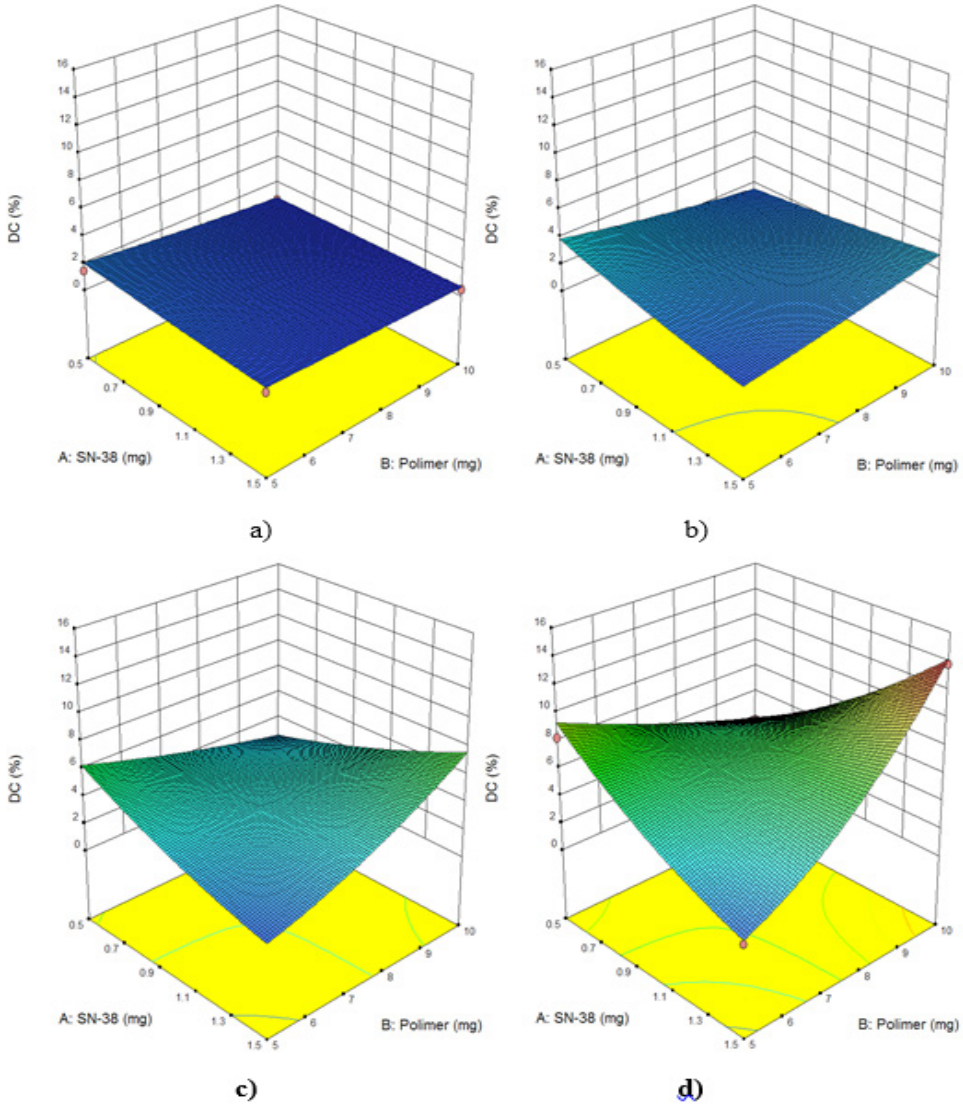

Figure 6. Response 3D Surface Plot for drug content with square root transformation at different concentration levels of Lutrol F127: a) 1%, b) 2.%, c) 3%, d) 4%.

When F127=1% (low setting), the contour plot reveals little. All DC values are less than 2%. Increasing F127 to 2% shows an increase in DC. At this setting, the highest results are either with both SN-38 and Polymer P(DL)LCL at their lowest settings or with both SN-38 and Polymer P(DL)LCL at their highest settings. When F127=3%, the DC response increases further. The optimal setting here is at SN-38=1.5 mg and Polymer P(DL)LCL =10 mg. Predicted DC is just over 7%. The optimal values for DC appear to be at F127=4%, SN-38=1.5 mg and Polymer P(DL)LCL =10 mg (all values at highest settings): predicted DC is approximately 14%, as presented in figures 5 and 6.

Particle size (PS)

ANOVA (Table III) shows that, of the main effects, only SN-38 has a statistically significant effect on size. However, polymer P(DL)LCL has a p-value of 0.0589 so although not statistically significant at the 5 mg, it clearly has an important effect.

Two-factor interactions AC is statistically significant (p=0.0123), suggesting that the effect of SN-38 depends on the setting of F127 (and vice versa). There appears to be no statistical evidence for interactions between SN-38 and Polymer P(DL)LCL or Polymer P(DL)LCL and F127. The three-factor interaction ABC is not statistically significant (p=0.1962).

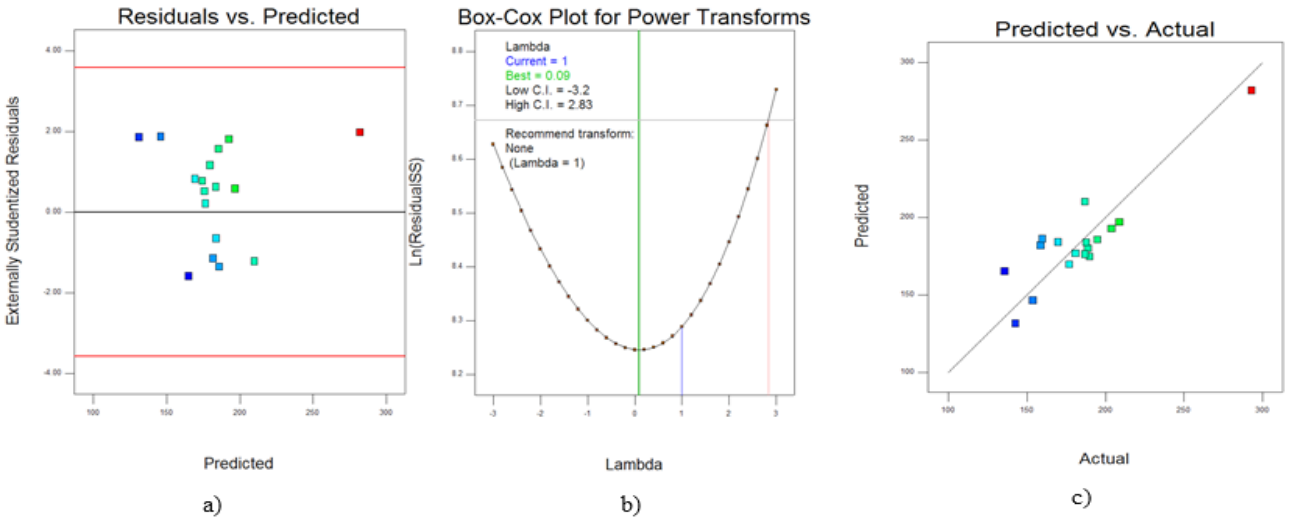

Figure 7. Response for particle size a) Residuals vs Predicted chart, b) Box-Cox plot, c) Predicted vs Actual chart.

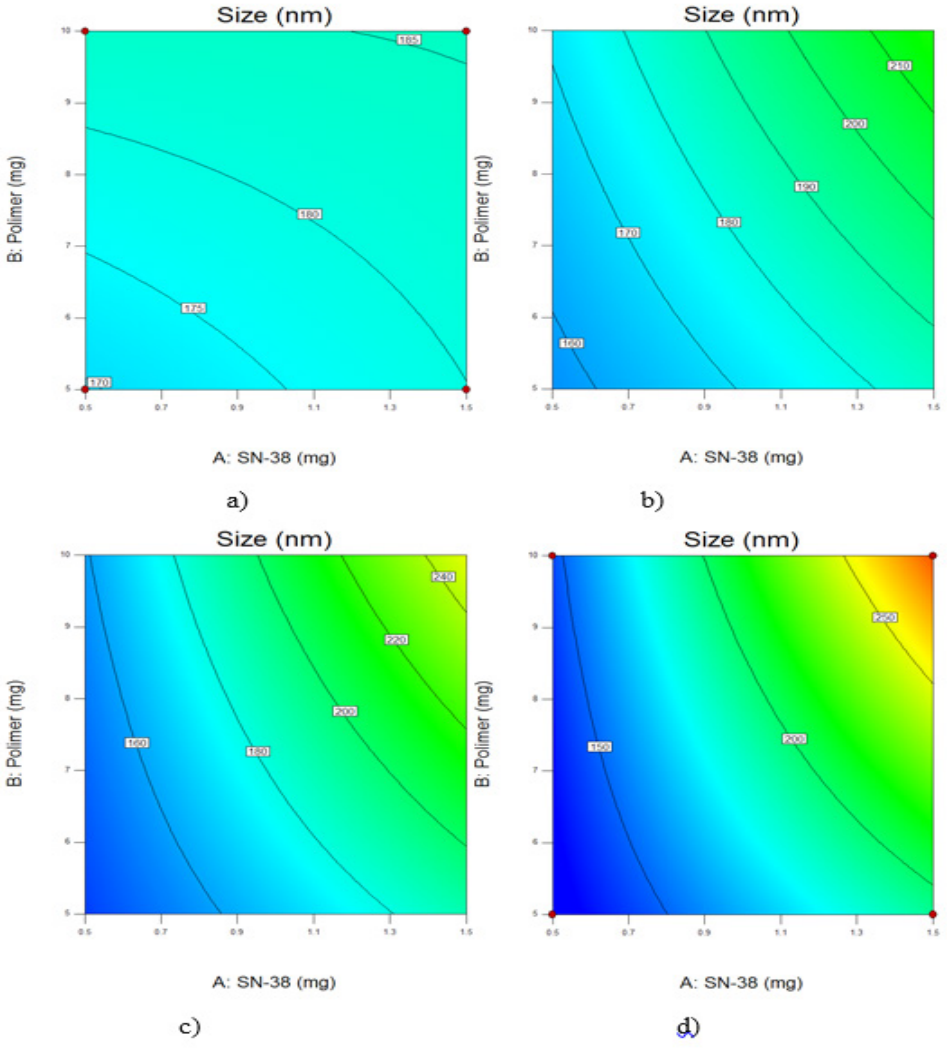

Figure 8. Response Contour Plot for particle size at different concentration levels of Lutrol F127: a) 1%, b) 2.%, c) 3%, d) 4%.

The most statistically important effects on size can be identified by looking for those with the smallest p-values: main effect SN-38 and 2FI AC.

Looking at the F-Values (a.k.a Signal / Noise ratio) shows that the effect of SN-38 is approximately 15 times greater than the estimated background noise.

The Adjusted R-Squared value is less than the R-Squared value, and in this case, the difference of <0.2 gives little cause for concern.

A large difference between Predicted R-Squared and the other R-Squared metrics indicates that this model may not give as good predictions as we'd ideally like.

The Residuals vs Predicted chart for response PS (Figure 7) shows that there appear to be no potential outliers. For response size, the Box-Cox Plot has identified no transformation that would provide a better model fit. This plot provides a visual indication of how well the fitted model is able to predict the observed experimental results (a perfect model would result in all points appearing on the line). In this case the model appears to give reasonably good predictions on average, although observations appear to be systematically under- /over-predicted.

When F127=1% (low setting), the contour plot reveals little. All size values are less than 190 nm. Increasing F127 to 2% shows a decrease in size (Figure 8 and 9). At this setting, the lowest results are with both SN-38 and polymer P(DL)LCL at their lowest settings where predicted Size is just below 160 nm. When F127=3%, the Size response decreases further. The optimal setting here is again at low SN-38 and low polymer. Predicted size is approximately 145 nm. The optimal values for drug content appear to be at F127=4%, SN-38=0.5mg and polymer=5 mg and predicted size is approximately 130 nm.

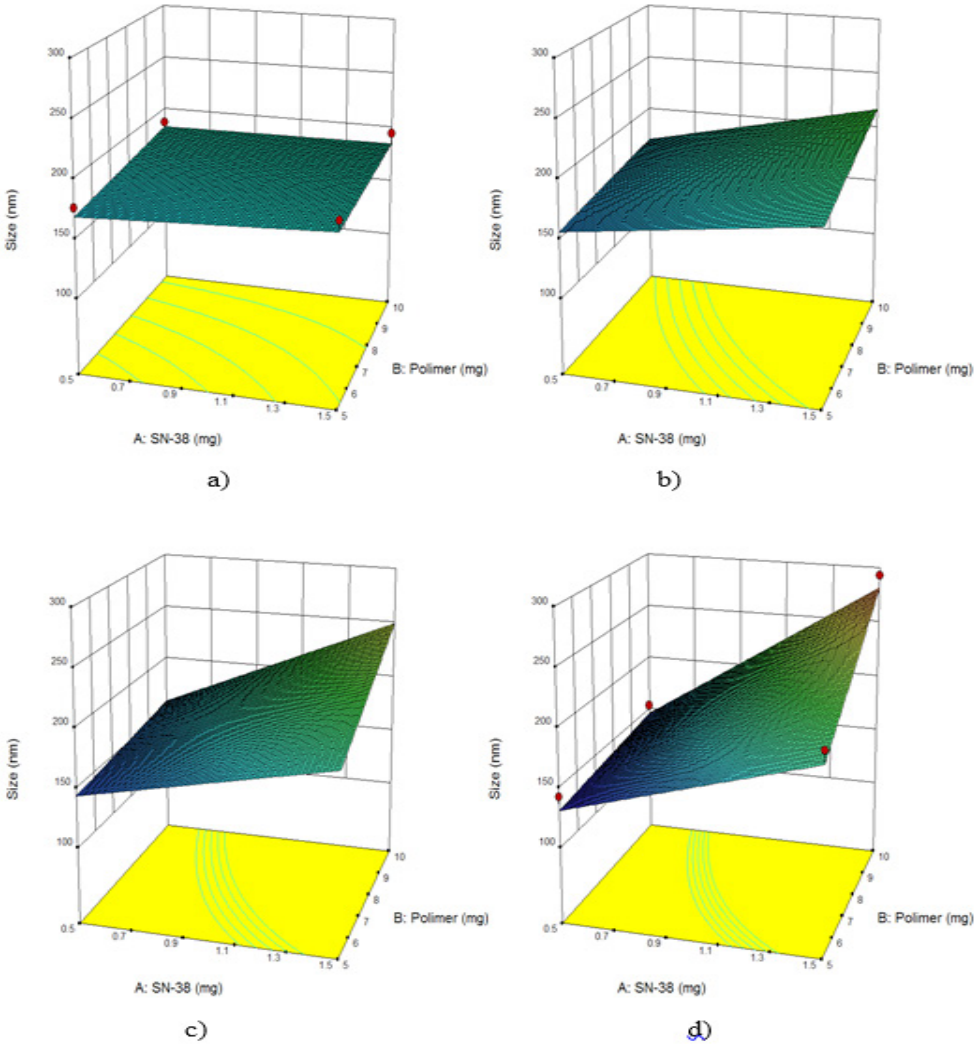

Figure 9. Response 3D Surface Plot for particle size with at different concentration levels of Lutrol F127 a) 1%, b) 2.%, c) 3%, d) 4%.

Numerical Optimization

Using the models constructed in the previous analysis steps, optimal factor settings have been identified and gave the desired performance. The optimization criteria were defined as follows:

Response	Goal
EE	Maximize
DC	Maximize
Size	Minimize (<200 nm)

As presented in the results, the models for EE and DC use the models fitted to the transformed data (Square Root transform in both cases).

Multiple solutions were found; the 15 most desirable are shown at table IV. The most desirable solution is shown visually via Design-Expert's "Ramps" report, at figure 10.

Table IV. Desirable solutions.

Constraints						
Name	**Goal**	**Lower Limit**	**Upper Limit**	**Lower Weight**	**Upper Weight**	**Importance**
A: SN-38	is in range	0.5	1.5	1	1	3
B: Polymer	is in range	5	10	1	1	3
C: F127	is in range	1	4	1	1	3
EE	maximize	2.42	92.06	1	1	3
DC	maximize	0.456	13.8	1	1	3
Size	maximize	136	200	1	1	3

Solutions							
Number	**SN-38**	**Polymer**	**F127**	**EE**	**DC**	**Size**	**Desirability**
1	0.5	5	4	87.533	9.38	131.431	0.86
2	0.5	5.02	4	87.476	9.353	131.49	0.858
3	0.5	5.047	4	87.398	9.317	131.571	0.857
4	0.5	5	3.986	87.083	9.334	131.606	0.857
5	0.5	5.089	4	87.281	9.263	131.694	0.855
6	0.507	5	4	86.619	9.304	131.844	0.854
7	0.5	5.11	4	87.221	9.235	131.757	0.854
8	0.5	5.155	4	87.093	9.176	131.89	0.851
9	0.518	5	4	85.166	9.185	132.504	0.845
10	0.5	5	3.93	85.278	9.148	132.316	0.844
11	0.5	5.324	4	86.614	8.955	132.393	0.843
12	0.521	5	3.998	84.568	9.134	132.773	0.842
13	0.5	5.002	3.915	84.773	9.095	132.519	0.841
14	0.5	5.362	4	86.509	8.907	132.503	0.841
15	0.53	5	4	83.464	9.045	133.286	0.835

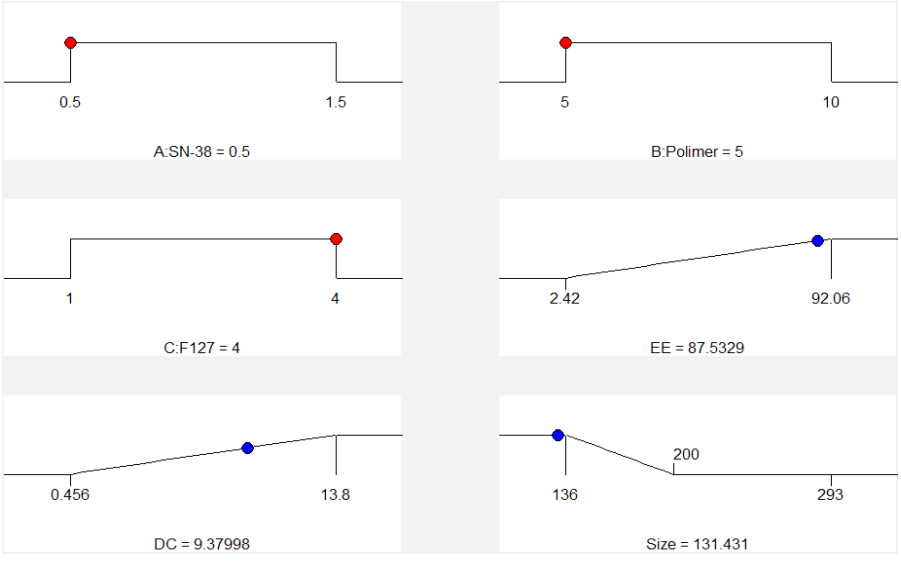

Figure 10. Optimized solution via Design-Expert's.

This shows that, according to the response goals specified above, the most desirable combination of factor settings is SN-38=0.5 mg, Polymer=5mg and F127=4%. These results predicted values of approximately EE=88%, DC=9.4% and Size=131 nm.

Discussion and conclusion

The successful scale-up and manufacturing of a nanomedicine present unique challenges in pharmaceutical development. Since most nanoparticles are complex multicomponent products with specific arrangement of components, a full understanding of the components and their interactions is essential to defining the key characteristics of the product, such as drug content, encapsulation efficacy and particles size, respectively. Identifying these characteristics early in development in turn, greatly helps define larger scale manufacturing in order to establish critical process steps and analytical criteria that ensure reproducibility of the product.

Nanoprecipitation might be a very limiting process for efficacious incorporation of extremely hydrophobic substances SN-38 into a hydrophobic core P(DL)LCL with passive drug loading mechanisms. Statistical analysis confirmed that drug content was mostly influenced by the amount of F-127. Also, due to very low solubility of SN-38, there is a limit (or small range around the limit) concentration of the drug substance into the medium for nanoprecipitation that will provide efficacious encapsulation. The limit concentration is highly dependent upon the stabilizing agent concentration, as F-127 actually helps the solubilisation of the drug during the process of nanoprecipitation. Having in mind the mentioned influence of the formulation factors and their interactions upon nanoparticles properties, we used the experimental design and found the optimal conditions to assemble PEO-PPO-PEO/P(DL)LCL particles as carriers of SN-38, with loading capacity 9.4%, encapsulation efficacy 88% and size 131 nm.

References

1. Singh AP, Biswas A, Shukla A, Maiti P. Targeted therapy in chronic diseases using nanomaterial-based drug delivery vehicles. Signal Transduct Target Ther. 2019;4:33.
2. Bulbake U, Doppalapudi S, Kommineni N, Khan W. Liposomal Formulations in Clinical Use: An Updated Review. Pharmaceutics. 2017;9:12.
3. Sevastre AS, Horescu C, Baloi SC, Cioc CE, Vatu BI, Tuta C, et al. Benefits of Nanomedicine for Therapeutic Intervention in Malignant Diseases. Coatings. 2019;9:628.
4. Feng SS, Mu L, Win KY, Huang G. Nanoparticles of biodegradable polymers for clinical administration of paclitaxel. Curr Med Chem. 2004;11:413-424.
5. Rovira-Bru M, Thompson DH, Szleifer I. Size and structure of spontaneously forming liposomes in lipid/PEG-lipid mixtures. Biophys J. 2002;83:2419-2439.
6. Rai R, Alwani S, Badea I. Polymeric Nanoparticles in Gene Therapy: New Avenues of Design and Optimization for Delivery Applications. Polymers (Basel). 2019;11:745.
7. Vauthier C, Bouchemal K. Methods for the preparation and manufacture of polymeric nanoparticles. Pharm Res. 2009;26:1025-1058.
8. Nel A, Xia T, Mädler L, Li N. Toxic potential of materials at the nanolevel. Science. 2006;311:622-627.
9. Song Y, Li X, Du X. Exposure to nanoparticles is related to pleural effusion, pulmonary fibrosis and granuloma. Eur Respir J. 2009;34:559-567.
10. Soares S, Sousa J, Pais A, Vitorino C. Nanomedicine: Principles, Properties, and Regulatory Issues. Front Chem. 2018;6:360.
11. Mourdikoudis S, Pallares RM, Thanh NT. Characterization techniques for nanoparticles: comparison and complementarity upon studying nanoparticle properties. Nanoscale. 2018;10:12871-12934.
12. Cagliani R, Gatto F, Bardi G. Protein Adsorption: A Feasible Method for Nanoparticle Functionalization? Materials (Basel). 2019;12:1991.
13. Nandhakumar S, Dhanaraju MD, Sundar VD, Heera B. Influence of surface charge on the in vitro protein adsorption and cell cytotoxicity of paclitaxel loaded poly(ε-caprolactone) nanoparticles. Bulletin of Faculty of Pharmacy, Cairo University. 2017;55:249-258.
14. Park JT, Seo JA, Ahn SH, Kim JH, Kang SW. Surface modification of silica nanoparticles with hydrophilic polymers. J Ind Eng Chem. 2010;16:517-522.
15. Müller RH. Colloidal carriers for controlled drug delivery and targeting: Modification, characterization and in vivo distribution. Taylor & Francis, 1991;119.
16. Pearson RM, Juettner VV, Hong S. Biomolecular corona on nanoparticles: a survey of recent literature and its implications in targeted drug delivery. Frontiers in chemistry. 2014;2:108.
17. Neagu M, Piperigkou Z, Karamanou K, Engin AB, Docea AO, Constantin C, et al. Protein bio-corona: critical issue in immune nanotoxicology. Arch Toxicol. 2017;91:1031-1048.
18. Chenthamara D, Subramaniam S, Ramakrishnan SG, Krishnaswamy S, Essa MM, Lin FH, et al. Therapeutic efficacy of nanoparticles and routes of administration. Biomater Res. 2019;23:20.
19. Bodratti AM, Alexandridis P. Formulation of Poloxamers for Drug Delivery. J Funct Biomater. 2018;9:11.
20. Benhabbour SR, Sheardown H, Adronov A. Protein resistance of PEG-functionalized dendronized surfaces: effect of PEG molecular weight and dendron generation. Macromolecules. 2008 Jul 8;41(13):4817-4823.
21. Fang C, Shi B, Pei YY, Hong MH, Wu J, Chen HZ. In vivo tumor targeting of tumor necrosis factor-α-loaded stealth nanoparticles: effect of MePEG molecular weight and particle size. Eur J Pharm Sci. 2006;27:27-36.
22. Bazile D, Prud'homme C, Bassoullet MT, Marlard M, Spenlehauer G, Veillard M. Stealth Me.PEG-PLA

nanoparticles avoid uptake by the mononuclear phagocytes system. J Pharm Sci. 1995;84:493-498.

23. Stolnik S, Illum L, Davis SS. Long circulating microparticulate drug carriers. Adv Drug Deliv Rev. 2012;64:290-301.
24. Zahr AS, Davis CA, Pishko MV. Macrophage uptake of core-shell nanoparticles surface modified with poly(ethylene glycol). Langmuir. 2006;22:8178-8185.
25. Stolnik S, Dunn SE, Garnett MC, Davies MC, Coombes AG, Taylor DC, et al. Surface modification of poly(lactide-co-glycolide) nanospheres by biodegradable poly(lactide)-poly(ethylene glycol) copolymers. Pharm Res. 1994;11:1800-1808.
26. Fam SY, Chee CF, Yong CY, Ho KL, Mariatulqabtiah AR, Tan WS. Stealth Coating of Nanoparticles in Drug-Delivery Systems. Nanomaterials (Basel). 2020;10:787.
27. Parmar K, Patel JK. Surface Modification of Nanoparticles to Oppose Uptake by the Mononuclear Phagocyte System. In Pathak Y, eds. Surface Modification of Nanoparticles for Targeted Drug Delivery Springer, Cham, 2019. p. 221-236.
28. Damodaran VB, Fee CJ, Ruckh T, Popat KC. Conformational studies of covalently grafted poly(ethylene glycol) on modified solid matrices using X-ray photoelectron spectroscopy. Langmuir. 2010;26:7299-7306.
29. Damodaran VB, Fee CJ, Popat KC. Prediction of protein interaction behaviour with PEG-grafted matrices using X-ray photoelectron spectroscopy. Appl Surf Sci. 2010;256:4894-901.
30. Suk JS, Xu Q, Kim N, Hanes J, Ensign LM. PEGylation as a strategy for improving nanoparticle-based drug and gene delivery. Adv Drug Deliv Rev. 2016;99(Pt A):28-51.
31. Walkey CD, Olsen JB, Guo H, Emili A, Chan WC. Nanoparticle size and surface chemistry determine serum protein adsorption and macrophage uptake. J Am Chem Soc. 2012;134:2139-2147.
32. Gref R, Lück M, Quellec PF, Marchand MF, Dellacherie EF, Harnisch SF, et al. 'Stealth' corona-core nanoparticles surface modified by polyethylene glycol (PEG): influences of the corona (PEG chain length and surface density) and of the core composition on phagocytic uptake and plasma protein adsorption. Colloids Surf B Biointerfaces. 2000;18:301-313.
33. Turecek PL, Bossard MJ, Schoetens F, Ivens IA. PEGylation of Biopharmaceuticals: A Review of Chemistry and Nonclinical Safety Information of Approved Drugs. J Pharm Sci. 2016;105:460-475.
34. Tagami T, Nakamura K, Shimizu T, Yamazaki N, Ishida T, Kiwada H. CpG motifs in pDNA-sequences increase anti-PEG IgM production induced by PEG-coated pDNA-lipoplexes. J Control Release. 2010;142:160-166.
35. Abu Lila AS, Doi Y, Nakamura K, Ishida T, Kiwada H. Sequential administration with oxaliplatin-containing PEG-coated cationic liposomes promotes a significant delivery of subsequent dose into murine solid tumor. J Control Release. 2010;142:167-173.
36. Ishida T, Atobe K, Wang X, Kiwada H. Accelerated blood clearance of PEGylated liposomes upon repeated injections: effect of doxorubicin-encapsulation and high-dose first injection. J Control Release. 2006;115:251-258.
37. Zhong Z, Rosenow M, Xiao N, Spetzler D. Profiling plasma extracellular vesicle by pluronic block-copolymer based enrichment method unveils features associated with breast cancer aggression, metastasis and invasion. J Extracell Vesicles. 2018;7:1458574.
38. Li JT, Caldwell KD. Plasma protein interactions with Pluronic™-treated colloids. Colloid Surface B. 1996;7:9-22.
39. Tavares MR, de Menezes LR, Dutra Filho JC, Cabral LM, Tavares MI. Surface-coated polycaprolactone nanoparticles with pharmaceutical application: Structural and molecular mobility evaluation by TD-NMR. Polymer Testing. 2017;60:39-48.
40. Linley S, Thomson NR, McVey K, Sra K, Gu FX. Influence of Pluronic coating formulation on iron oxide nanoparticle transport in natural and oil-impacted sandy aquifer media. Can J Chem Eng. 2020;98:642-649.
41. Palacio J, Agudelo NA, Lopez BL. PLA/pluronic® nanoparticles as potential oral delivery systems: Preparation, colloidal and chemical stability, and loading capacity. J Appl Polym Sci. 2016;133:43828.
42. Wu Z, Guo C, Liang S, Zhang H, Wang L, Sun H, et al. A pluronic F127 coating strategy to produce stable up-conversion NaYF4: Yb, Er (Tm) nanoparticles in culture media for bioimaging. J Mater Chem. 2012;22:18596-18602.
43. Rybak-Smith M.J. Effect of Surface Modification on Toxicity of Nanoparticles. In: Bhushan B. eds. Encyclopedia of Nanotechnology. Springer, Dordrecht 2016 p. 940-947.
44. Cheung S, O'Shea DF. Directed self-assembly of fluorescence responsive nanoparticles and their use for real-time surface and cellular imaging. Nat Commun. 2017;8:1885.
45. Lundqvist M, Augustsson C, Lilja M, Lundkvist K, Dahlbäck B, Linse S, et al. The nanoparticle protein corona formed in human blood or human blood fractions. PLoS One. 2017;12:e0175871.
46. Moghimi SM, Muir IS, Illum L, Davis SS, Kolb-Bachofen V. Coating particles with a block co-polymer (poloxamine-908) suppresses opsonization but permits the activity of dysopsonins in the serum. Biochim Biophys Acta. 1993;1179:157-165.
47. Santander-Ortega MJ, Jódar-Reyes AB, Csaba N, Bastos-González D, Ortega-Vinuesa JL. Colloidal stability of pluronic F68-coated PLGA nanoparticles: a variety of stabilisation mechanisms. J Colloid Interface Sci. 2006;302:522-529.